Clays and Clay Minerals, Vol. 48, No. 1, 95–105, 2000.

MINERALOGICAL AND Rb-Sr ISOTOPE STUDIES OF LOW-TEMPERATURE DIAGENESIS OF LOWER CAMBRIAN CLAYS OF THE BALTIC PALEOBASIN OF NORTH ESTONIA

KALLE KIRSIMÄE[1] AND PER JØRGENSEN[2]

[1]Institute of Geology, University of Tartu, Vanemuise 46, 51014 Tartu, Estonia
[2]Department of Soil and Water Sciences, Agricultural University of Norway, B.P. 5028, 1432 Aas, Norway

Abstract—X-ray diffraction (XRD), Rb-Sr isotope analysis, transmission electron microscopy (TEM), energy-dispersive X-ray spectroscopy (EDS), and Fourier transform infrared (FTIR) methods were used to study diagenetic illite and illite-smectite (I-S) in Lower Cambrian unlithified clays of shallow depth of burial in the northern part of the intercratonic Baltic paleosedimentary basin of the East-European Platform. The studies focused on the <0.06-μm size fraction of the clay. This fraction consists of a highly illitic illite-smectite (I-S) and a poorly crystalline illite (PCI), with some traces of Fe-rich chlorite also present. Rb-Sr isotopic data for the <0.06-μm size fractions suggest that the illitic I-S and PCI have different formation ages. No precise isotopic ages were derived directly owing to the composite illite mineralogy and retention of radiogenic Sr. This retention occurred because of imperfect isotopic homogenization at low water/rock ratios. The age of burial diagenesis is proposed to coincide with the time of maximum burial depth, which was achieved during the Middle to Late Devonian and continued until Permian-Triassic erosion. Because of the shallow depth of burial (<2 km), diagenesis was probably a low-temperature (<50°C) transformation process. The resident time of 100–150 million years at maximum burial had a major influence in the process.

Key Words—Baltic Paleosedimentary Basin, Cambrian, Low-Temperature Diagenesis, Illitization.

INTRODUCTION

Over the last three decades, smectite illitization involving the illite-smectite (I-S) mixed-layer transitional phases has been one of the most studied diagenetic processes in argillaceous sedimentary sequences (Powers, 1967; Burst, 1969; Hower *et al.*, 1976; Boles and Franks, 1979; Nadeau *et al.*, 1985; Ahn and Peacor, 1986; Freed and Peacor, 1989; Eberl, 1993). However, the factors controlling the transition are still not entirely understood.

Assuming primarily a temperature-controlled transformation, various empirical I-S geothermometers were utilized (*e.g.*, Hoffman and Hower, 1979; Pytte and Reynolds, 1989; Pollastro, 1993). However, an inconsistency between smectite proportions and temperature (burial depth) is frequently observed (Lahann, 1980; Velde *et al.*, 1986; Freed and Peacor, 1989; Buatier *et al.*, 1992; Li *et al.*, 1995). Essene and Peacor (1995) noted that chemical disequilibrium of the smectite to illite reactions excludes their use as a measure of the absolute temperature. Thus, the smectite to illite transformation apparently depends on time-temperature factors (Velde and Espitalié, 1989) with other factors contributing to the control of the reaction kinetics: rock/water ratio (Whitney, 1990), fluid and rock composition (Huang *et al.*, 1993), starting composition of the I-S (Freed and Peacor, 1989; Pollastro, 1990), and the presence of organic compounds (Small, 1994).

In the northern part of the Baltic sedimentary paleobasin of the East-European Platform, the unmetamorphosed nature of the entire section of the Vendian to Devonian sediments, including Lower Cambrian unlithified clayey sediments, implies a very stable tectonic history and shallow burial of sediments for >500 million years. Although the Lower Cambrian sediments are considered as almost diagenetically unchanged (Pirrus, 1970, 1983; Rozanov and Łydka, 1987), others have noted that clay-mineral diagenesis has indeed occurred (Reier, 1965, 1967; Firsov *et al.*, 1971). The important role of diagenetic processes affecting minerals at low temperature, particularly I-S and illite, was shown by Gorokhov *et al.* (1994) and Kirsimäe *et al.* (1999a). The clay fraction was found consisting of detrital $2M_1$ mica/illite, diagenetic $1M'_d$ illite, and mixed-layer I-S formed ~50–150 million years after deposition.

This study focuses on improving our knowledge of the mineralogical-chemical composition and age of formation of the sediments affected by diagenesis. These sediments do not have detectable detrital impurities in the finest fraction (<0.06 μm) and are unlikely to have experienced temperatures >50°C.

GEOLOGICAL SETTING AND MATERIALS

The section of the Lower Cambrian sediments studied is located in the northernmost part of the Baltic paleosedimentary basin, on the southern slope of the Baltic (Fennoscandian) Shield (Figure 1). In the Lower Cambrian succession, with a thickness of ~150 m in north Estonia, unlithifed clays and silty clays belonging to the Lontova/Voosi and Lükati formations pre-

Copyright © 2000, The Clay Minerals Society

https://doi.org/10.1346/CCMN.2000.0480112 Published online by Cambridge University Press

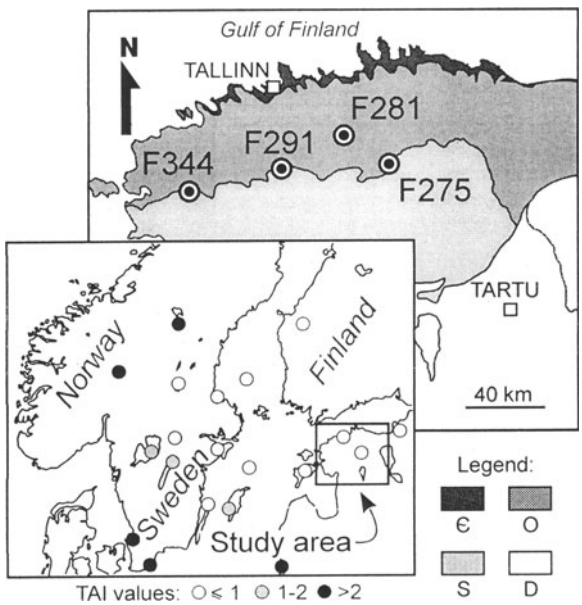

Figure 1. Location of the boreholes studied and the regional geology of Estonia. Legend: Є - Cambrian; O - Ordovician; S - Silurian; D - Devonian. Acritarch thermal-alteration data (TAI, Hayes *et al.*, 1983) shown on inset are from Hagenfeldt (1996), Talyzina (1998), and Ivo Paalits (pers. comm., 1998).

vail. Thick-bedded, coarse-grained siltstones of the Tiskre Formation occur only in the uppermost part of the section (Mens and Pirrus, 1997a) (Figure 2). Authigenic minerals (glauconite, chemogenic phosphate, pyrite) and fossil assemblages suggest that the sediments were deposited under normal marine conditions (Mens and Pirrus, 1986). Geological data on the well-characterized paleogeography and lithology of the Vendian and Cambrian terrigenous sediments on the East-European Platform, including the Baltic Paleobasin, are summarized by Rozanov and Łydka (1987) and Mens and Pirrus (1997a, 1997b). The sediments are traditionally correlated to Lower Cambrian Tommotian and Atabanian age: 534–524 million years ago (Ma) (Mens *et al.*, 1990; Gradstein and Ogg, 1996). However, there is strong evidence supporting an older age (545–530 Ma), Nemakit-Daldynian and Tommotian, of these sediments (Moczydłowska and Vidal, 1988; Volkova *et al.*, 1990).

The sediment lithology is characterized by the high content of a <2-μm fraction, exceeding 40–45% of the sediment, and a natural-water content of 8–28% (Kirsimäe *et al.*, 1999b; Pirrus and Saarse, 1979). The <0.06-μm fraction, studied in this work, constitutes ≤25% of the clay fraction. We use the terms "clay" and "silty-clay" to emphasize the unlithified nature of these sediments.

In the clay fraction (<2 μm), illite and I-S are the dominating phases (>70%), followed by kaolinite and

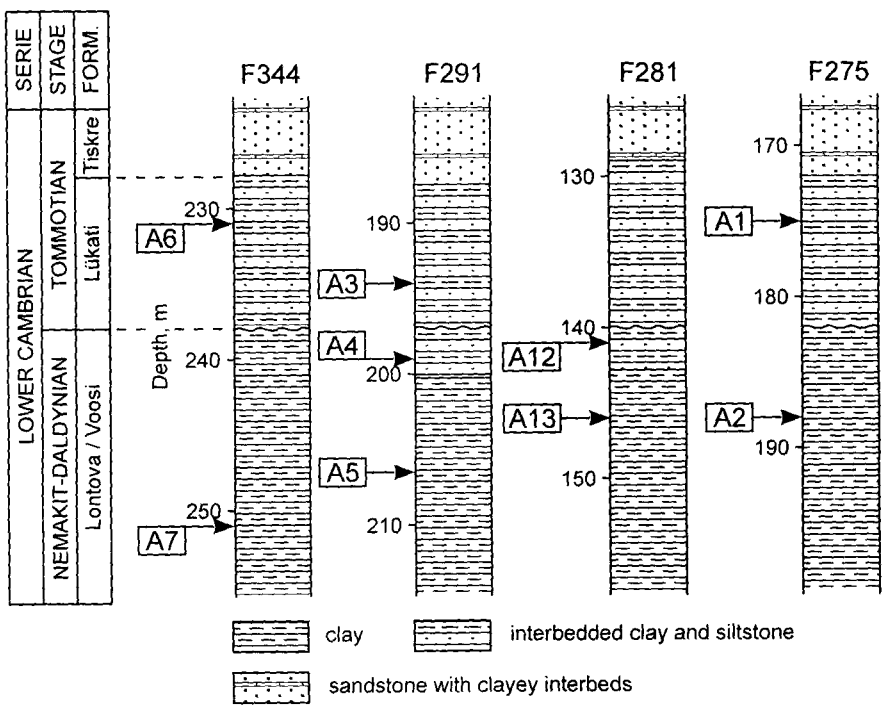

Figure 2. Stratigraphic columns for Lower Cambrian and the schematic lithological sections of the boreholes with samples depths.

https://doi.org/10.1346/CCMN.2000.0480112 Published online by Cambridge University Press

chlorite. Some quartz and K-rich feldspar (orthoclase) with traces of hematite/pyrite, albite, and dolomite are also present (Gorokhov *et al.,* 1994; Kirsimäe *et al.,* 1999b). The semiquantitative estimate of non-clay minerals content in the clay fraction (<2 μm) is on average <20% and it increases to 60–75% in the 2–6-μm fraction. Quartz is the most abundant among the non-clay minerals, whereas the orthoclase content varies from 5–10 to 15–25% in <2-μm and 2–6-μm fractions, respectively (Kirsimäe *et al.,* 1999b). K_2O content (wt. %) in whole rock and in the <2-μm fraction varies narrowly from 4.4 to 5.4% and from 6.2 to 7.1%, respectively (Mens and Pirrus, 1977; Kirsimäe *et al.,* 1999b). The content of presumably detrital mica and/or well-crystallized illite as well as kaolinite and chlorite decreases with decreasing grain size in fractions from 2 to <0.06 μm. The <0.06-μm fraction was found by Kirsimäe *et al.* (1999a) to consist only of diagenetically formed illitic minerals.

Kirsimäe *et al.* (1999a) found a Rb-Sr age of 860 Ma for detrital mica and orthoclase in coarse-size fractions. Consequently, they assumed that material from the weathering and erosion of the mainly mafic high-grade metamorphic rocks of Sveconorwegian age (1100–900 Ma) in southwestern Scandinavia was an important source for the Early Cambrian sediments. In addition, weathering of the widespread Upper Proterozoic and Lower Cambrian basaltic rocks on the western margin of the East-European Platform in Poland, Belarus, Russia, the Ukraine, and Moldova, with an age of 551 Ma (Compston *et al.,* 1995) could have contributed a mostly smectitic clay component to the Early Cambrian intercratonic shallow sea on the East-European Platform.

The samples collected from four wells (Figures 1 and 2) are representative for the latitudinal distribution of the Lower Cambrian clayey sediments in north Estonia. Both major lithological units, the Lükati and Lontova/Voosi Formations, were sampled.

METHODS

Cleaned, air-dried, drill-core samples were dispersed in distilled water without any crushing, grinding, or other additional pretreatment. A few mL of 4% hexametaphosphate were added and a brief ultrasonic treatment was used to improve particle separation. The <2-μm fraction was separated using standard sedimentation procedures, whereas the <0.06-μm particles were separated by ultracentrifugation. Suspensions containing the <0.06-μm fraction were flocculated and subsequently saturated with 1 N NaCl. Salt excess was removed by repeated washing with distilled water and ethanol. X-ray diffraction (XRD) data were collected using oriented clay-aggregate samples obtained by smearing clay paste onto glass slides. A DRON-3M diffractometer with Ni-filtered CuKα radiation, two 1.5° soller slits, 0.5-mm divergence, and 0.25-mm receiving slits was used. The relative humidity during experiments was 60–65%. The scanning steps were 0.02 °2θ and counting time was 2 or 3 s per step. The XRD curves were obtained in an air-dry (AD) state and after treatment in ethylene glycol (EG) vapor for 48 h at 60°C.

Background-stripped XRD curves were decomposed in the 5–12 °2θ region according to the models proposed by Lanson and Champion (1991), Lanson and Velde (1992), and Lanson (1997), with AXES code (Mändar *et al.,* 1996). No smoothing was used prior to decomposition. A Gaussian peak-shape model for poorly crystallized illite (PCI) and I-S phases and a Lorenzian-shape model for chlorite traces were used for both AD and EG XRD curve decomposition.

The Fourier transform infrared (FTIR) spectra in the OH-stretching region were obtained with a Perkin-Elmer Paragon 500 FTIR spectrometer. Slides were made by drying a drop of the dilute <0.06-μm clay suspension on an IR transparent IRTRAN-2 window. Most adsorbed water was removed with heating at 120°C for 16 h. An absorption spectrum was obtained from 64 scans with a resolution of 1 cm^{-1} in the 4000–700-cm^{-1} region. A reference spectrum of the IRTRAN-2 window and the atmospheric background, recorded at the same conditions prior to the sample analysis, was subtracted automatically by the system software.

For observations by transmission electron microscope (TEM) and energy-dispersive X-ray (EDS) analyses, air-dry, fine fractions were dispersed in ethanol. A drop of dilute alcohol suspension was transferred onto a Cu grid covered by a holey carbon film. Evaporated samples were investigated in a JEM 200CX TEM equipped with a Tracor Northern TN2000 EDS analyser at 200 kV. EDS spectra were quantitatively evaluated using modified Tracor Northern software with experimentally derived *k*-ratios.

Rb-Sr isotope analyses were performed on the <0.06-μm Na^+-exchanged clay at the Laboratory of Isotope Geology, University of Oslo with a VG 354 mass spectrometer. Rb and Sr concentrations of the 0.05-g samples were analyzed by isotope dilution. The errors are estimated at ±2% for the $^{87}Rb/^{86}Sr$ ratios and ±0.00020 (2σ) for the $^{87}Sr/^{86}Sr$ ratios. The measured $^{87}Sr/^{86}Sr$ ratio of the NBS 987 standard was 0.710162 ± 0.000012 (2σ). The decay constant for ^{87}Rb used in the age calculations is 1.42×10^{-11} y^{-1} (Steiger and Jäger, 1977).

RESULTS

XRD analysis of the <0.06-μm fraction show that the major components are I-S, PCI, and occasionally some Fe-rich chlorite (Figure 3). The PCI corresponds to illite particles with a small coherent scattering domain size (CSDS) with <5% of expandability (Lanson and Champion, 1991). No XRD-detectable detrital

https://doi.org/10.1346/CCMN.2000.0480112 Published online by Cambridge University Press

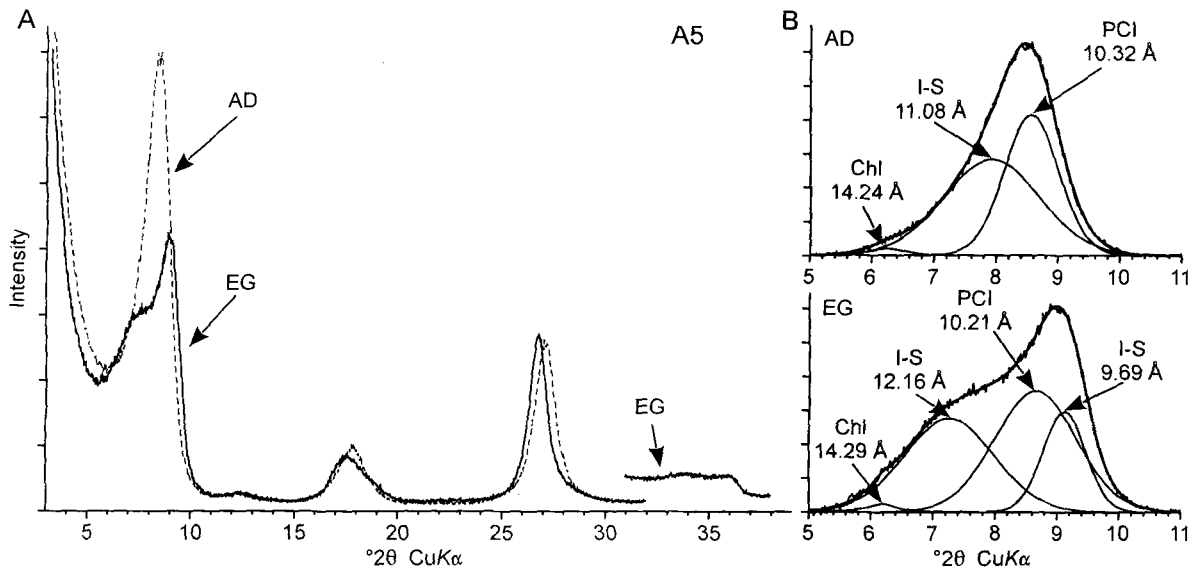

Figure 3. XRD patterns for sample A5 (<0.06-μm fraction) in air-dry (AD) and ethylene glycol-solvated (EG) state. Before (A) and after (B) background stripping and decomposition. Chl - chlorite; I-S - interstratified illite-smectite; PCI - poorly crystallized illite with a small coherent scattering domain and <5% of expandability.

mica or illite or orthoclase was found in the <0.06-μm fraction.

In an earlier study, Kirsimäe *et al.* (1999a) interpreted from the decomposition of XRD peaks the possibility of two I-S phases with 30–45% and <15% smectite layers, respectively. However, an inconsistency between the AD and EG XRD curves was noted and a possibility of a single I-S phase was discussed.

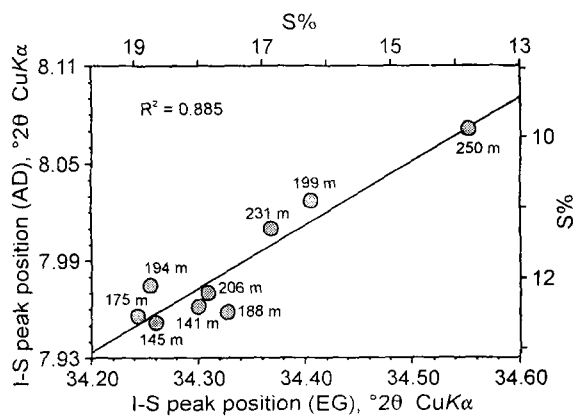

Figure 4. Correlation between the content of smectite layers in illite-smectite (S%) determined from the position of the decomposed I-S low-angle (5–9°) peak in an air-dry (AD) state and determined from the peak position in 33–35 °2θ region after ethylene glycol solvation (EG). S% scale for the EG sample is from Środoń (1984). S% for the AD sample was found from low-angle peak position of ordered (R 1.5) I-S minerals in AD state calculated using the NEWMOD code (Reynolds, 1985) assuming $4 \leq N \geq 7$ distribution of coherent layers (see text for details). Numbers on the graph show burial depth of the samples today.

A critical reexamination of previous and new XRD curves suggests a single I-S population coexisting with PCI. This is also supported by reasonable consistency between decomposed AD and EG curves showing mixtures of two illitic populations: expandable (I-S) and practically non-expandable (PCI) (Figure 3). However, PCI peak widening and a peak-maxima shift towards higher angles in the EG treated curves (Figure 3) may indicate an expandability of ~5%. Limitations of the decomposition method do not permit discrimination between PCI low-angle peaks in the EG curve owing to small angular differences and close full width at half maximum (FWHM) values (Lanson, 1997).

Expandability (S%) of the I-S, estimated with the procedure of Środoń (Figure 7 in Środoń, 1984), is 14–19% (±4%). By comparing EG curves modeled from NEWMOD (Reynolds, 1985), we find that the R (Reichweite) type of I-S ordering is $1 \leq R \geq 2$. Decomposed AD curves were used to determine I-S low-angle peak positions. A plot of these values in a "S% - Peak position" diagram, obtained from low-angle peak positions of R (1.5) ordered I-S minerals based on NEWMOD (Reynolds, 1985) shows 4–6% less smectite. However, the results from these smectite determinations are well correlated, as illustrated in Figure 4, and smectite estimates according to AD curves match within error (±4%) of the smectite estimate after EG treatment. Theoretical I-S XRD curves for AD were calculated, assuming a CSDS distribution with $4 \leq N \geq 7$, where N is the number of elementary layers, illite $d(001)$ = 9.98 Å, and smectite $d(001)$ = 14 Å for Na^+-saturated samples. In contrast, S% estimated from theoretical I-S AD curves assuming smectite

https://doi.org/10.1346/CCMN.2000.0480112 Published online by Cambridge University Press

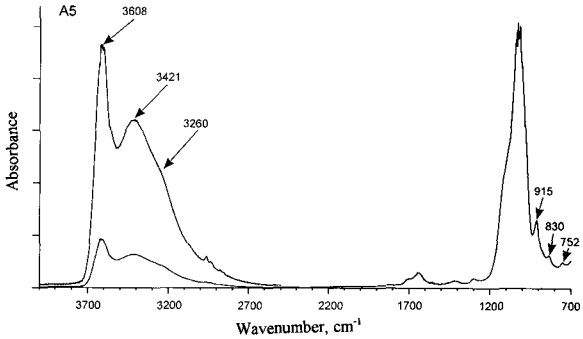

Figure 5. FTIR spectrum of an oriented film of the <0.06-μm fraction.

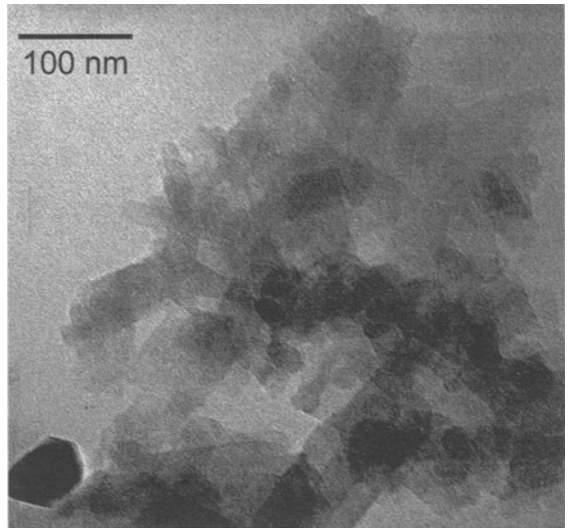

Figure 6. TEM image of the <0.06-μm clay fraction. The thick well defined euhedral crystallite in the left lowermost corner is probably Fe-chlorite.

d(001) = 12.5 Å (hydration with one-water layer in the interlayer) is overestimated by only 1–3% compared with the EG treatment. Moore and Hower (1986) suggested a 12.5-Å spacing after determining d(001) = 12.4 Å for Na-rich smectite at 60–65% relative humidity, which matches with our experimental conditions. However, according to Sato *et al.* (1992), d(001)-values for Na-rich smectite varie between 12.45–14.98 Å at 60% relative humidity. Large d(001)-values of near 15 Å for Na-rich smectite occur if most part of the layer charge is from octahedral-site substitutions. Moreover, the S% in I-S estimated from selected Mg^{2+}-saturated samples (AD) of <0.06-μm size fractions is within ±1% of the data of Na^{+}-saturated samples, assuming d(001) for smectite for NEWMOD models at 15 and 14 Å for Mg and Na varieties, respectively.

Although the present uncorrected burial depth for our samples varies only from 141 to 250 m below ground surface, there is an indication that the S% in the I-S decreases with increasing sample depth (Figure 4).

The FTIR absorption spectra of the <0.06-μm size fractions confirm the dioctahedral illitic composition, but the spectra are characterized by a broad, poorly resolved OH-stretching band at 3600–3621 cm^{-1}. This partly overlaps with the OH-stretching bands of adsorbed water at 3421 and 3260 cm^{-1}. Weak diagnostic OH-bending vibration frequencies at 830 and 752 cm^{-1} (Figure 5) resemble a typical phengitic illite (Russel, 1987). The well-resolved Al-Al-OH bending frequency at 915 cm^{-1}, in combination with a stretching frequency at 3600–3621 cm^{-1}, is characteristic of dioctahedral illite and smectite (Borchardt, 1977; Russel, 1987).

The TEM study of the <0.06-μm size fraction reveals only tangentially overlapping lath-shaped illitic crystallites with short dimensions varying from ~20 to 50 nm and long dimensions ~50 to ≥100 nm (Figure 6). Occasionally, high-contrast grains with an euhedral shape and well-defined edges occur. These grains are probably chlorite (Figure 6). The dimensions of lath-shaped particles are in good agreement with the fraction limit (0.06 μm = 60 nm) calculated from centrifugation parameters.

EDS results of single grains were not of acceptable quality owing to the very small dimensions of individual particles, and we analyzed aggregates of partly overlapping laths. Qualitative chemical data presented as crystallochemical formulae are given in Table 1. Structural formulae are based on 22 negative charges per $O_{10}(OH)_2$. All Fe was taken as Fe(II), although XRD analyses of coarser fractions (Kirsimäe *et al.*, 1999a, 1999b) showed that some samples contain minor hematite, which may buffer the iron in the sediment to a ferric state. Ferric iron in these sediments is also observed by the sediment color variations from greenish-gray to occasionally reddish-violet. Red has been interpreted (Mens and Pirrus, 1986) as the "primary" sediment color, and it was preserved owing to the lack of organic material required for iron reduction.

The composition of these laths is similar to the high charge Fe, Mg-rich illite (highly illitic I-S) typically found in diagenetic environments (Meunier and Velde, 1989; Lanson and Champion, 1991; Środoń *et al.*, 1992; Freed and Peacor, 1992; Ransom and Helgeson, 1993; Hover *et al.*, 1996). The Fe content in illite and illite-rich I-S can be overestimated owing to traces of Fe-rich chlorite in the same fraction, but since the amount is nearly the same for all samples, no attempt was made to correct for possible Fe-rich chlorite impurities.

The Rb-Sr isotopic-composition data of nine <0.06-μm separates are shown in Table 2. The apparent isotope age was estimated using isochrone-plot and mod-

https://doi.org/10.1346/CCMN.2000.0480112 Published online by Cambridge University Press

Table 1. EDS analysis of illite-rich illite-smectite and illite particles in the <0.06-μm fraction of samples A3, A5, A7, and A13 converted into structural formulae based on $O_{10}(OH)_2$. Deviations shown are derived from counting statistics (Ch = charge).

Sample/ analysis	K	Mg	Fe(II)	^{VI}Al	Ch. (VI)	^{IV}Al	Si	Ch. (IV)
A3-1	0.63 ± 0.03	0.21 ± 0.05	0.30 ± 0.02	1.57 ±0.06	−0.26	0.38 ± 0.01	3.62 ± 0.07	−0.38
A3-2	0.77 ± 0.02	0.24 ± 0.03	0.32 ± 0.01	1.50 ± 0.04	−0.39	0.38 ± 0.01	3.62 ± 0.05	−0.38
A3-3	0.71 ± 0.01	0.16 ± 0.02	0.27 ± 0.01	1.58 ± 0.02	−0.41	0.29 ± 0.00	3.71 ± 0.03	−0.29
A3-4	0.72 ± 0.05	0.23 ± 0.09	0.25 ± 0.03	1.69 ± 0.08	0.03	0.75 ± 0.03	3.25 ± 0.10	−0.75
A3-5	0.63 ± 0.01	0.14 ± 0.02	0.27 ± 0.01	1.61 ± 0.02	−0.32	0.30 ± 0.00	3.70 ± 0.03	−0.30
A5-1	0.81 ± 0.02	0.18 ± 0.04	0.34 ± 0.01	1.48 ± 0.04	−0.53	0.28 ± 0.01	3.72 ± 0.05	−0.28
A5-2	0.67 ± 0.02	0.34 ± 0.04	0.45 ± 0.01	1.36 ± 0.04	−0.33	0.34 ± 0.01	3.66 ± 0.05	−0.34
A5-3	0.57 ± 0.01	0.15 ± 0.02	0.20 ± 0.01	1.61 ± 0.03	−0.47	0.10 ± 0.00	3.90 ± 0.04	−0.10
A5-4	0.76 ± 0.02	0.16 ± 0.03	0.21 ± 0.01	1.69 ± 0.04	−0.20	0.56 ± 0.01	3.44 ± 0.05	−0.56
A7-1	0.91 ± 0.01	0.17 ± 0.02	0.43 ± 0.01	1.40 ± 0.02	−0.58	0.38 ± 0.01	3.62 ± 0.03	−0.38
A7-2	0.90 ± 0.02	0.16 ± 0.03	0.33 ± 0.01	1.48 ± 0.03	−0.58	0.32 ± 0.01	3.68 ± 0.04	−0.32
A7-3	0.71 ± 0.01	0.24 ± 0.02	0.33 ± 0.01	1.51 ± 0.02	−0.34	0.37 ± 0.01	3.63 ± 0.03	−0.37
A7-4	0.78 ± 0.01	0.13 ± 0.03	0.30 ± 0.01	1.54 ± 0.03	−0.51	0.28 ± 0.01	3.72 ± 0.04	−0.28
A7-5	0.78 ± 0.01	0.17 ± 0.02	0.30 ± 0.01	1.55 ± 0.03	−0.41	0.37 ± 0.01	3.63 ± 0.03	−0.37
A13-1	0.69 ± 0.02	0.26 ± 0.02	0.37 ± 0.01	1.45 ± 0.03	−0.38	0.31 ± 0.01	3.69 ± 0.03	−0.31
A13-2	0.90 ± 0.03	0.20 ± 0.04	0.39 ± 0.02	1.41 ± 0.05	−0.57	0.33 ± 0.01	3.67 ± 0.06	−0.33
A13-3	0.68 ± 0.02	0.26 ± 0.03	0.35 ± 0.01	1.48 ± 0.03	−0.35	0.33 ± 0.01	3.67 ± 0.04	−0.33

el-age calculations. The best-fit line through all the $^{87}Sr/^{86}Sr$ and $^{87}Rb/^{86}Sr$ data is a possible isochron with an intercept at 0.69377 ± 0.00544 and a determined isochrone age of 533 ± 41 Ma (Figure 7, line A). The initial $^{87}Sr/^{86}Sr$ ratio of this single isochron is unreasonably low and close to the initial value for the solar system. Plotting the data on a $^{87}Sr/^{86}Sr$ *vs.* 1/Sr graph also reveals a poor-quality linear correlation which is compatible with a mixing of phases with different radiogenic ages. Alternatively, the isochrone plot can be interpreted with four samples of lowest $^{87}Sr/^{86}Sr$ and $^{87}Rb/^{86}Sr$ ratios. This fits a line that represents a second "isochron" (Figure 7, line B), yielding an age of 278 ± 40 Ma with a high initial $^{87}Sr/^{86}Sr$ ratio of 0.74621 ± 0.00862. The remaining five points fit with a line (Figure 7, line C), with a still unreasonably low initial intercept at 0.69981 ± 0.00502 and an age of 518 ± 17 Ma. These alternative results are also in dispute.

Table 2. Rb-Sr analytical data and I-S/PCI ratio in the <0.06-μm fraction. Model ages are calculated using an assumed initial $^{87}Sr/^{86}Sr$ ratio of 0.7085 (Kaufmann *et al.*, 1996). I-S and PCI contents were determined from the areas of decomposed low-angle XRD peaks and normalized to 100%.

Sample	Rb, ppm	Sr, ppm	$^{87}Sr/^{86}Sr$	$^{87}Rb/^{86}Sr$	Model age, Ma	I-S/PCI, wt. %
A1	156.81	36.19	0.79507	12.65	481	62/38
A2	156.82	21.29	0.85944	21.63	490	60/40
A3	143.41	29.06	0.80560	14.41	473	63/37
A4	167.62	24.08	0.85106	20.43	490	61/39
A5	161.76	21.21	0.86586	22.41	493	59/41
A6	133.07	24.91	0.80708	15.61	443	65/35
A7	151.70	25.53	0.82904	17.40	486	60/40
A12	166.57	27.97	0.81475	17.41	428	61/39
A13	158.69	27.97	0.84247	19.50	482	58/42

DISCUSSION AND CONCLUSION

Geologically meaningful ages of the composite illitic minerals in sediments are often difficult to obtain directly from Rb-Sr isochrone-plots. Alternatively, Rb-Sr model ages were calculated assuming an initial Sr isotope ratio of 0.7085 (marine Sr ratio of Early Cambrian from Kaufman *et al.*, 1996). All model ages (Table 2) of the studied samples are considerably younger than the single "isochron" age (Figure 7, line A). Most of the results fall narrowly between 473–493 Ma, but two samples, A6 and A12, have an apparent model age of 443 and 428 Ma, respectively.

The relationship between the apparent Rb-Sr model ages and the I-S/PCI ratio (Table 2), suggests that there

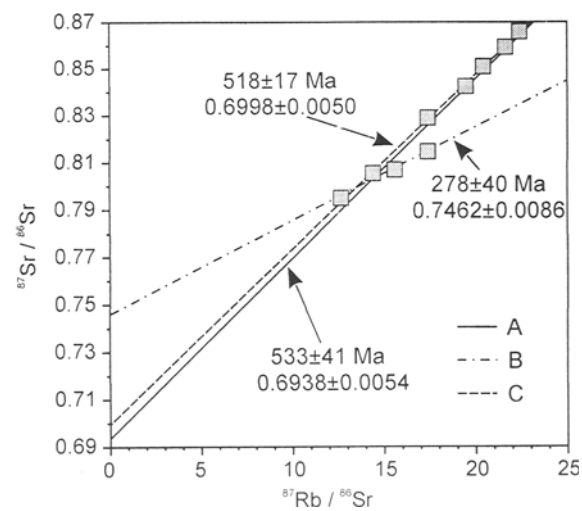

Figure 7. Rb-Sr isotopic data for the <0.06-μm fractions. See text for explanation of A, B, and C "isochrons".

https://doi.org/10.1346/CCMN.2000.0480112 Published online by Cambridge University Press

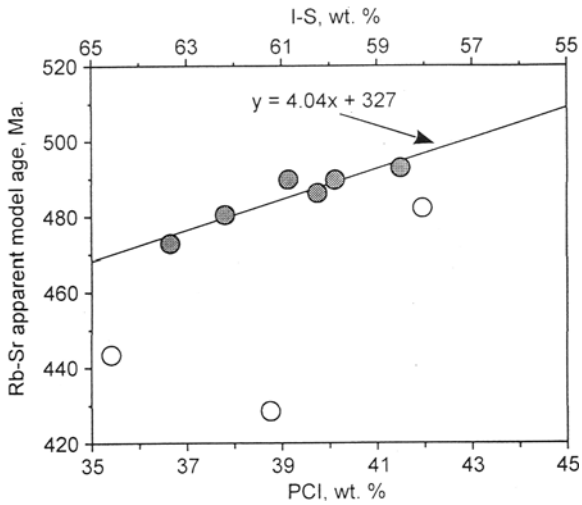

Figure 8. Relationship between the Rb-Sr apparent model ages and the I-S and discrete PCI content in the <0.06-μm fraction. Model ages were calculated assuming an initial $^{87}Sr/^{86}Sr$ ratio of 0.7085 (Kaufman *et al.*, 1996). Shaded samples were used for end-members age interpolation.

are different isotopic ages for two illitic phases in the <0.06-μm fraction (Figure 8). The I-S and PCI content in the <0.06-μm fraction was found from a decomposed low-angle (5–9 °2θ) peak of AD I-S and *d*(001) integrated-peak areas of PCI calculated to 100%. The Rb-Sr model ages appear to increase with an increasing I-S/PCI ratio, except for three points which lie off the line on Figure 8. The remaining six points indicate that the <0.06-μm fraction consists of an isotopically older PCI population and of a younger I-S population, mixed in various proportions. Extrapolation of ages towards possible end-members using these six samples, suggests an isotope age of 327 Ma for the I-S population and 731 Ma for the PCI population. However, the initial $^{87}Sr/^{86}Sr$ ratio for these populations was possibly different from Early Cambrian seawater and only during early diagenesis would the diagenetic fluids and sea water have the same Sr isotope ratio. Moreover, the samples that do not plot on the line on Figure 8 indicate a more complex composition of the fraction caused by either mixing of several phases with different origin, or inhibited isotopic equilibration during diagenesis. This is supported by XRD and EDS analyses (Tables 1 and 2). The XRD data show coexistence of two apparent illitic minerals and the EDS analyses can be divided into two groups with different K contents, but similar composition of the octahedral sites. We believe that the chemical data is explained by mixing two end-members, illite and highly illitic I-S, although distinctions in particle shape cannot be made and the EDS results are averaged over many particles.

The Lower Cambrian clays outcrop at the northern margin of the Baltic paleobasin and the burial depth increases slowly (2.5–3.5 m km^{-1}) southwards to >2000 m depth in southeastern Lithuania. In northern Estonia, the present day burial depth is within a few hundred meters (Figure 2). The XRD characteristics of the illitic materials, however, suggest a much higher diagenetic grade of the sediments normally attained at burial depths of several kilometers. Nevertheless, Kirsimäe *et al.* (1999a) concluded from geological data that the maximum burial depth for the Lower Cambrian clay in northern Estonia did not exceed ~800–1000 m and a maximum temperature of ~35°C, assuming a constant thermal gradient of 20°C km^{-1}. Shallow burial and low paleotemperatures are also indicated by the unconsolidated lithology of the sediments and by the unaltered microfossil organic material in these and stratigraphically nearby sediments. Studies of thermal alteration of acritarchs (Talyzina, 1998), conodonts (Männik and Viira, 1990), and cithinozoas (Jaak Nõlvak, pers. comm., 1998) suggest maximum paleotemperatures ≤50°C. The latter is supported by a systematic study on thermal alteration of conodonts (CAI index of Epstein *et al.*, 1977) in Ordovician rocks in Scandinavia and adjacent areas (Bergström, 1980). CAI values decrease to 1–1.5 (temperatures ≤80°C) in eastern Sweden, adjacent to the study area. A similar pattern, with decreasing acritarch thermal-alteration indexes (TAI, Hayes *et al.*, 1983) was shown by Hagenfeldt (1996) for the Lower Palaeozoic (Cambrian through Silurian). In western Finland and in eastern Sweden, TAI values of 1(1+) indicate paleotemperatures of <50°C and a total thickness of Palaeozoic sediments of only 1600 m (Figure 1) occurred. More recently, Felitsyn *et al.* (1998) reported CAI values of 1–1.5 in the Upper Cambrian to Lower Ordovician sediments from northern Estonia and northwestern Russia (St. Petersburg area).

The maximum burial in Scandinavia and probably also in the northwestern part of the East-European Platform occurred in Late Silurian to late Middle Devonian at ~430–380 Ma. In south-central Scandinavia, a thickness of ~3 km for the Silurian-Devonian, mostly terrigenous, sediments was estimated by Hagenfeldt (1996). Apatite fission-track data from the crystalline basement showed that the Silurian-Devonian cover in Scandinavia was nearly uneroded until the Permian-Triassic period, and then it was denudated for ~80 million years (Tullborg *et al.*, 1995). The same burial history can be assumed for the northern part of the Baltic paleobasin, which is characterized by a somewhat slower sedimentation rate and a thinner sediment cover.

Early Cambrian sedimentation in the northern part of the Baltic paleobasin was followed by a period of ~25–30 million years, when episodic sparse sedimentation and denudation occurred under alternating marine and continental conditions (Mens and Pirrus, 1997b). According to the paleohydrogeological mod-

https://doi.org/10.1346/CCMN.2000.0480112 Published online by Cambridge University Press

els of Mokrik (1997), the marine connate waters in the Vendian-Cambrian sediments in this area were displaced by an unsaturated meteoric-freshwater influx during this latter period. This influx could cause partial dissolution of detrital orthoclase, plagioclase, and mica in the more permeable silty-sandy inter-layers of the Lower Cambrian sequence. Hypothetically, the excess K^+ released in this process may have activated the first episode of illitization in the sediments. If so, then "isochron" C (Figure 7) with an age of 518 ± 17 Ma, may be a result of this event. A similar Rb-Sr isochron age, with a scattering between 522–505 Ma was found for the <0.1-μm size fractions of the Lontova unit by Gorokhov *et al.* (1994). The only difference is the very low initial $^{87}Sr/^{86}Sr$ value of ~0.69981 in our study. Although this low $^{87}Sr/^{86}Sr$ ratio may be caused by undersaturated meteoric water equilibrating with mostly basaltic or basic gneiss detritus, strong evidence suggests a mixed isochron.

The development of the basin continued with a very slow terrigenous-sedimentation rate during the end of the Late Cambrian (Mens and Pirrus, 1997b), followed by carbonate sedimentation in the Ordovician and Silurian (Nestor and Einasto, 1997). The mixed terrigenous-carbonate sedimentation during Devonian resulted in a maximum burial in the northern Baltic paleobasin probably in late Middle to early Late Devonian (380–360 Ma, Kuršs, 1992). The "isochron" B (Figure 7) with an age of 278 ± 40 Ma falls approximately in this period with maximum burial before the Permian-Triassic denudation. Consequently, further illitization, in this case forming the highly illitic I-S, may be tentatively interpreted as a result of basin subsidence and increasing burial depths reaching maximum temperatures of only ~50°C. This occurred over a long period (100–150 million years) under slowly reactive conditions. The end of this period of maximum burial coincides with extensive rifting and graben system development in the Oslo area, the North Sea, and adjacent areas in the western part of the Baltic Shield (Ziegler, 1982). Areas of igneous activity in association with the Oslo rifting with an age of 305–240 Ma (Sundvoll *et al.,* 1990), are known eastward from the active Oslo rift only in central Sweden and in the southern Baltic Sea, ~500–600 km to the southwest and west from the study area (Puura *et al.,* 1991). However, Larson and Tullborg (1998) showed that the U-Pb concordia lower-intercept ages of zircon from Precambrian rocks of the Baltic Shield indicate late Paleozoic (350–200 Ma) age. They concluded that the radiogenic Pb loss and subsequent Pb deposition in basement fractures is related to long-term leaching by low-temperature hydrothermal solutions originating from meteoric-water circulation (thermal convection) during late Palaeozoic burial beneath a thick sedimentary cover. A similar limited Pb-Zn mineralization associated with metasomatic dolomitization during late Palaeozoic or possibly Permian (Väino Puura, pers. comm., 1998), is known from fractured zones in Ordovician-Silurian carbonate sequences in the northern part of the Baltic paleobasin. Since the extent of illitization in our clays does not seem to vary significantly with distance from known fracture zones, this dolomitization and subsequent sulphide mineralization had no substantial influence on the clay-mineral diagenesis in the low-permeable sediments. There is no geological evidence on further diagenesis after the Permian-Triassic erosion. Tectonically stable continental conditions were prevailing and further burial diagenesis was inhibited after this erosion.

In summary, the diagenetic Rb-Sr ages from two "isochrons" B and C (Figure 7) are consistent with known geological history. This suggests that there are two distinct crystallization episodes and our samples (<0.06-μm size fractions) are mixtures of phases formed in these episodes. Thus, the apparent sample ages calculated from these "isochrons" and the content of phases in the binary mixture should plot on a straight line interpolating the ages close to both hypothetical end-members (*e.g.,* Mossmann, 1991). However, the scatter of data prevents this interpolation. Also, the initial $^{87}Sr/^{86}Sr$ ratios of the "isochrons" are unrealistically low (0.69981) or high (0.74621). Therefore, we conclude that for illitic clay (<0.06-μm size fraction) free of detectable detrital impurities, reliable age(s) for diagenesis cannot be obtained directly from Rb-Sr data. This result is related to limited isotopic homogenization during low-temperature (<50°C) diagenesis in the Late Devonian to Permian. Low permeability of the homogenous sediments probably inhibited isotopic equilibration of the metastable intermediate I-S and possible end-member illite (PCI) during diagenesis. A mixed-isotopic system of clay and the high apparent isotopic age of the PCI found from Rb-Sr model ages may also be explained by a solid-state transformation mechanism of smectite-to-illite evolution. A strict solid-state transformation mechanism would allow the retention of radiogenic daughter isotopes in the crystal structure during transformation (Altaner and Ylagan, 1997). Therefore, the end-member illite (PCI) appears isotopically older than the precursor I-S. In addition, a solid-state transformation mechanism of smectite-to-illite would involve a lower activation-energy barrier compared to a dissolution-precipitation mechanism (Cuadros and Linares, 1996) and consequently the transformation will be kinetically favored.

ACKNOWLEDGMENTS

We thank J. Jahren (University of Oslo) for help with TEM and EDS analyses, and J. Nõlvak (Technical University of Tallinn), I. Paalits (University of Tartu), and S. Hagenfeldt (University of Stockholm) for unpublished data on thermal alteration of cithinozoas and acritarchs. Discussions with V. Puura were important contributions. The Estonian Geological

https://doi.org/10.1346/CCMN.2000.0480112 Published online by Cambridge University Press

Survey is thanked for providing samples, and the Amerada Hess Corporation and the Research Council of Norway for support of this work.

We are deeply indebted to J.J. Aronson, J.R. Mossman, and J. Środoń for significant improvement of the manuscript by their valuable reviews.

REFERENCES

Ahn, J.H. and Peacor, D.R. (1986) Transmission and analytical electron microscopy of the smectite-to-illite transition. *Clays and Clay Minerals,* **34,** 165–179.

Altaner, S.P. and Ylagan, R.F. (1997) Comparison of structural models of mixed-layer illite/smectite and reaction mechanisms of smectite illitization. *Clays and Clay Minerals,* **45,** 517–533.

Bergström, S.M. (1980) Conodonts as paleotemperature tools in Ordovician rocks of the Caledonides and adjacent areas in Scandinavia and the British Isles. *Geologiska Föreningens i Stockholm Förhandlingar,* **102,** 377–392.

Boles, J.F. and Franks, S.G. (1979) Clay diagenesis in Wilcox sandstones of southwest Texas, implications of smectite diagenesis on sandstone cementation. *Journal of Sedimentary Petrology,* **49,** 55–70.

Borchardt, G.A. (1977) Montmorillionite and other smectities minerals. In *Minerals in Soil Environments,* J.B. Dixon and S.B. Weed, eds., Soil Science Society of America, Madison, Wisconsin, 299–330.

Buatier, M.D., Peacor, D.R., and O'Neil, J.R. (1992) Smectite-illite transition in Barbados accretionary wedge sediments: TEM and AEM evidence for dissolution/crystallization at low temperature. *Clays and Clay Minerals,* **40,** 65–80.

Burst, J.F. (1969) Diagenesis of Gulf Coast clayey sediments and its possible relation to petroleum migration. *American Association of Petroleum Geologists Bulletin,* **53,** 73–93.

Compston, W., Sambridge, M.S., Reinfrank, R.F., Moczydłowska, M., Vidal, G., and Claesson, S. (1995) Numerical ages of volcanic rocks and the earliest faunal zone within the Late Precambrian of east Poland. *Journal of the Geological Society (London),* **152,** 599–611.

Cuadros, J. and Linares, J. (1996) Experimental kinetic study of the smectite-to-illite transformation. *Geochimica et Cosmochimica Acta,* **60,** 439–453.

Eberl, D.D. (1993) Three zones for illite formation during burial diagenesis and metamorphism. *Clays and Clay Minerals,* **41,** 26–37.

Epstein, A.G., Epstein, J.B., and Harris, L.D. (1977) *Conodont Color Alteration—An Index to Organic Metamorphism.* U.S. Geological Survey Professional Paper 995, Washington, D.C., 27 pp.

Essene, E.J. and Peacor, D.R. (1995) Clay mineral thermometry—a critical perspective. *Clays and Clay Minerals,* **43,** 540–553.

Felitsyn, S., Sturesson, U., Popov, L., and Holmer, L. (1998) Nd isotope composition and rare earth element distribution in early Paleozoic biogenic apatite from Baltoscandia: A signature of Iapetus ocean water. *Geology,* **26,** 1083–1086.

Firsov, L., Nikolajeva, I., Lebedev, Y., and Solntseva, S. (1971) Composition, origin and absolute age of micaceous minerals in Lower Cambrian blue clays of the Baltic Region. *Transactions of the Institute of Geology and Geophysics, Academy of Sciences of the USSR, Siberian Branch,* **144,** 165–192. (in Russian).

Freed, R.L. and Peacor, D.R. (1989) Variability in temperature of the smectite illite reaction in Gulf Coast sediments. *Clay Minerals,* **24,** 171–180.

Freed, R.L. and Peacor, D.R. (1992) Diagenesis and the formation of authigenic illite-rich I/S crystals in Gulf Coast Shales: TEM study of clay separates. *Journal of Sedimentary Petrology,* **62,** 220–234.

Gorokhov, I.M., Clauer, N., Turchenco, T.L., Melnikov, N.N., Kutyavin, E.P., Pirrus, E., and Baskakov, A.V. (1994) Rb-Sr systematics of Vendian-Cambrian claystones from the east European Platform: Implications for a multi-stage illite evolution. *Chemical Geology,* **112,** 71–89.

Gradstein, F.M. and Ogg, J. (1996) A Phanerozoic time scale. *Episodes,* **19,** 3–5.

Hagenfeldt, S. (1996) Lower Palaeozoic acritarchs as indicators of heat flow and burial depth of sedimentary sequences in Scandinavia. *Acta Universitatis Carolinae, Geologica,* **40,** 413–424.

Hayes, J.M., Kaplan, I.R., and Wedekning, K.M. (1983) Precambrian organic geochemistry, preservation of the record. In *Earth's Earliest Biosphere, its Origin and Evolution,* J.W. Schopf, ed., Princeton University Press, Princeton, 93–134.

Hoffman, J. and Hower, J. (1979) Clay minerals assemblages as low grade metamorphic geothermometers: Application to the thrust faulted disturbed belt of Montana, USA. *Society of Economic Paleontologists and Mineralogists Special Publication,* **26,** 55–79.

Hover, V.C., Peacor, D.R., and Lynn, M.W. (1996) STEM/AEM evidence for preservation of burial diagenetic fabrics in Devonian shales: Implications for fluid/rock interaction in cratonic basins (U.S.A.). *Journal of Sedimentary Research,* **66,** 519–530.

Hower, J., Eslinger, E.V., Hower, M.E., and Perry, E.A. (1976) Mechanisms of burial metamorphism of argillaceous sediment: 1. Mineralogical and chemical evidence. *Geological Society of America Bulletin,* **87,** 725–737.

Huang, W.L., Longo, J.M., and Pevear, D.R. (1993) An experimentally derived kinetic model for smectite-to-illite conversion and its use as a geothermometer. *Clays and Clay Minerals,* **41,** 162–177.

Kaufman, A.J., Knoll, A.H., Semikhatov, M.A., Grotzinger, J.F., Jacobsen, S.B., and Adams, W. (1996) Integrated chronostratigraphy of Proterozoic-Cambrian boundary beds in the Western Anabar region, Northern Siberia. *Geological Magazine,* **133,** 509–533.

Kirsimäe, K., Jørgensen, P., and Kalm, V. (1999a) Low temperature diagenetic illite-smectite in Lower Cambrian clays in North Estonia. *Clay Minerals,* **34,** 151–163.

Kirsimäe, K., Kalm, V., and Jørgensen, P. (1999b) Diagenetic transformation of clay minerals in Lower Cambrian argillaceous sediments of north Estonia. *Proceedings of the Estonian Academy of Sciences, Geology,* **48,** 15–34.

Kuršs, V. (1992) *Devonian Terrigenous Deposition on the "Main Devonian Field".* Zinatne, Riga, 216 pp. (in Russian).

Lahann, R.W. (1980) Smectite diagenesis and sandstone cement: The effect of reaction temperature. *Journal of Sedimentary Petrology,* **50,** 755–760.

Lanson, B. (1997) Decomposition of experimental X-ray diffraction patterns (profile fitting): A convenient way to study clay minerals. *Clays and Clay Minerals,* **45,** 132–146.

Lanson, B. and Champion, D. (1991) The I/S-to-illite reaction in the late stage diagenesis. *American Journal of Science,* **291,** 473–506.

Lanson, B. and Velde, B. (1992). Decomposition of X-ray diffraction patterns: A convenient way to describe complex I-S diagenetic evolution. *Clays and Clay Minerals,* **40,** 629–643.

Larson, S.-A. and Tullborg, E.-L. (1998) Why Baltic Shield zircons yield late Paleozoic, lower-intercept ages on U-Pb concordia? *Geology,* **26,** 919–922.

Li, G., Mauk, J.L., and Peacor, D.R. (1995) Preservation of clay minerals in the Precambrian (1.1 Ga) Nonesuch For-

https://doi.org/10.1346/CCMN.2000.0480112 Published online by Cambridge University Press

mation in the vicinity of the White Pine copper mine, Michigan. *Clays and Clay Minerals,* **43,** 361–370.

Mändar, H., Vajakas, T., Felche, J., and Dinnebier, R. (1996) AXES—a program for preparation of parameter input files for FULLPROF. *Journal of Applied Crystallography,* **29,** 304.

Männik, P. and Viira, V. (1990) Conodonts. In *Field Meeting Estonia 1990. An Excursion Guidebook,* D. Kaljo and H. Nestor, eds., Estonian Academy of Sciences, 84–90.

Mens, K. and Pirrus, E. (1977) *Stratotypes of the Cambrian Formations of Estonia.* Valgus, Tallinn, 68 pp. (in Russian).

Mens, K. and Pirrus, E. (1986) Stratigraphical characteristics and development of Vendian Cambrian boundary beds on the East European Platform. *Geological Magazine,* **123,** 357–360.

Mens, K. and Pirrus, E. (1997a) Cambrian. In *Geology and Mineral Resources of Estonia,* A. Raukas and A. Teedumäe, eds., Estonian Academy Publishers, Tallinn, 39–48.

Mens, K. and Pirrus, E. (1997b) Vendian-Tremadoc clastogenic sedimentation basins. In *Geology and Mineral Resources of Estonia,* A. Raukas and A. Teedumäe, eds., Estonian Academy Publishers, Tallinn, 184–191.

Mens, K., Bergström, J., and Lendzion, K. (1990). *The Cambrian System on the East-European Platform. Correlation Chart and Explanatory Notes.* International Union of Geological Sciences Publication No. 25, 73 pp.

Meunier, A. and Velde, B. (1989) Solid solutions in illite/smectite mixed layer minerals and illite. *American Mineralogist,* **74,** 1106–1112.

Moczydłowska, M. and Vidal, G. (1988) How old is Tommotian? *Geology,* **16,** 166–168.

Mokrik, R. (1997) *The Plaeohydrogeology of the Baltic Basin: Vendian and Cambrian.* Tartu University Press, Tartu, 138 pp.

Moore, D.M. and Hower, J. (1986) Ordered interstratification of dehydrated and hydrated Na-smectite. *Clays and Clay Minerals,* **34,** 379–384.

Mossmann, J.-R. (1991) K-Ar dating of authigenic illite-smectite clay material: Application to complex mixtures of mixed-layer assemblages. *Clay Minerals,* **26,** 189–198.

Nadeau, P.H., Wilson, M.J., McHardy, W.J., and Tait, J.M. (1985) The conversion of smectite to illite during diagenesis: Evidence from some illitic clays from bentonites and sandstones. *Mineralogical Magazine,* **49,** 393–400.

Nestor, H. and Einasto, R. (1997) Ordovician and Silurian carbonate sedimentation basin. In *Geology and Mineral Resources of Estonia,* A. Raukas and A. Teedumäe, eds., Estonian Academy Publishers, Tallinn, 192–204.

Pirrus, E. (1970) The distribution of clay minerals of Vendian and Cambrian deposits in east Estonia. *Eesti NSV Teaduste Akadeemia Toimetised, Keemia, Geoloogia,* **19,** 322–333. (in Russian).

Pirrus, E. (1983) The role of the palaeogeographic factor in the development of associations of clay minerals in Vendian and Cambrian basins in the north Baltic. In *Terrigenous Minerals of the Baltic Sedimentary Rocks,* H. Viiding, ed., Academy of Sciences, Estonian SSR, Institute of Geology, Tallinn, 76–91. (in Russian).

Pirrus, E. and Saarse, L. (1979) Geotechnical properties of the Cambrian clays in north Estonia. *Eesti NSV Teaduste Akadeemia Toimetised, Keemia, Geoloogia,* **28,** 68–74. (in Russian).

Pollastro, R. (1990) The illite/smectite geothermometry—Concepts, methodology, and application to basin history and hydrocarbon generation. In *Applications of Thermal Maturity Studies to Energy Exploration, Rocky Mountain Section,* V.F. Nuccio and C.E. Barker, eds., Society of Economic Paleontologists and Mineralogists, Tulsa, 1–18.

Pollastro, R. (1993). Considerations and applications of the illite/smectite geothermometer in hydrocarbon-bearing rocks of Miocene to Mississippian age. *Clays and Clay Minerals,* **41,** 119–133.

Powers, M.C. (1967). Fluid-release mechanisms in compacting marine mudrocks and their importance in oil exploration. *Bulletin of American Association of Petroleum Geologists,* **51,** 25–36.

Puura, V., Aliavdin, F., Amantov, A., and Korsakova, M. (1991) Intrusive formation. In *Geology and Geomorphology of the Baltic Sea,* A.A. Grigelis, ed., Nedra, Leningrad, 257–266. (in Russian).

Pytte, A.M. and Reynolds, R.C., Jr. (1989) The thermal transformation of smectite to illite. In *Thermal History of Sedimentary Basins: Methods and Case Histories,* N.D. Naeser and T.H. McCulloh, eds., Springer-Verlag, New York, 133–140.

Ransom, B. and Helgeson, H.C. (1993) Compositional end members and thermodynamic components of illite and dioctahedral aluminous smectite solid solutions. *Clays and Clay Minerals,* **41,** 537–550.

Reier, A. (1965) Mineralogical peculiarities of Cambrian clays of Estonian SSR. *Tallinna Polütehnilise Instuudi Toimetised,* **Serie A 221,** 3–11. (in Russian).

Reier, A. (1967) Authigenic minerals in clays of Lontova Formation. *Tallinna Polütehnilise Instituudi Toimetised,* **Serie A 246,** 19–25. (in Russian).

Reynolds, R.C., Jr. (1985) *NEWMOD, a computer program for the calculation of one-dimensional patterns of mixed-layered clays.* R.C. Reynolds, Jr., 8 Brook Rd., Hanover, New Hampshire.

Rozanov, A.Y. and Łydka, K., eds. (1987). *Palaeography and Lithology of the Vendian and Cambrian of the Western East-European Platform.* Wydawnictwa Geologiczne, Warsaw, 114 pp.

Russel, J.D. (1987) Infrared methods. In *A Handbook of Determinative Methods in Clay Mineralogy.* M.J. Wilson, ed., Chapman and Hall, New York, 133–173.

Sato, T., Takashi, W., and Otsuka, R. (1992) Effects of layer charge, charge location, and energy change on expansion properties of dioctahedral smectites. *Clays and Clay Minerals,* **40,** 103–113.

Small, J.S. (1994) Fluid composition, mineralogy and morphological changes associated with the smectite-to-illite reaction: An experimental investigation of the effect of organic acid anions. *Clay Minerals,* **29,** 539–554.

Środoń, J. (1984) X-ray powder diffraction identification of illitic minerals. *Clays and Clay Minerals,* **32,** 337–349.

Środoń, J., Elsass, F., McHardy, W.J., and Morgan, D.J. (1992) Chemistry of illite-smectite inferred from TEM measurements of fundamental particles. *Clay Minerals,* **28,** 137–158.

Steiger, R.H. and Jäger, E. (1977) Subcommision on geochronology: Convention on the use of decay constants in geo- and cosmochronology. *Earth and Planetary Science Letters,* **36,** 359–362.

Sundvoll, B., Neumann, E.-R., Larsen, B.T., and Tuen, E. (1990) Age relations among Oslo rift magmatic rocks: Implications for tectonic and magmatic modelling. *Tectonophysics,* **178,** 67–87.

Talyzina, N.M. (1998) Fluorescence intensity in Early Cambrian acritarchs from Estonia. *Review of Paleobotany and Palynology,* **100,** 99–108.

Tullborg, E.-L., Larson, S.-Å., Björklund, L., Samuelsson, L., and Stigh, J. (1995) *Thermal Evidence of Caledonide Foreland, Molasse Sedimentation in Fennoscandia.* Svensk Kärnbränslehantering AB Technical Report 95-18, Swedish

https://doi.org/10.1346/CCMN.2000.0480112 Published online by Cambridge University Press

Nuclear Fuel and Waste Management Co., Stockholm, 38 pp.

Velde, B. and Espitaliè, J. (1989) Comparison of kerogen maturation and illite/smectite composition in diagenesis. *Journal of Petroleum Geology,* **12,** 103–110.

Velde, B., Suzuki, T., and Nicot, E. (1986) Pressure-temperature composition of illite/smectite mixed-layer minerals: Niger Delta mudstones and other examples. *Clays and Clay Minerals,* **34,** 435–441.

Volkova, N.A., Kiryanov, V.V., Piskun, L.V., and Rudavskaya, V.A. (1990) All-Union colloquium on Precambrian and Lower Palaeozoic acritarchs. *Geologicheskij Zhurnal,* **6,** 132–133. (in Russian).

Whitney, G. (1990) The role of the water in the smectite to illite reaction. *Clays and Clay Minerals,* **38,** 343–350.

Ziegler, P.A. (1982) *Geological Atlas of Western and Central Europe.* Shell Internationale Petroleum Maatschappij B.V., Elsevier, Amsterdam, 130 pp.

E-mail of corresponding author: arps@math.ut.ee

(*Received 2 September 1998; accepted 28 July 1999; Ms. 98-110*)

https://doi.org/10.1346/CCMN.2000.0480112 Published online by Cambridge University Press